# Monte Carlo treatment of resonance-radiation imprisonment in fluorescent lamps

J. B. Anderson
*Department of Chemistry, The Pennsylvania State University, 152 Davey Laboratory, University Park, Pennsylvania 16802*

J. Maya, M. W. Grossman, R. Lagushenko, and J. F. Waymouth
*GTE Lighting Products Division, 100 Endicott Street, Danvers, Massachusetts 01923*
(Received 26 October 1984)

The imprisonment of the 2537-Å resonance radiation from mercury in the mercury-argon discharge of fluorescent lamps is treated by a Monte Carlo method. The effects of emission and absorption linewidths, hyperfine splitting, isotopic composition, collisional transfers of excitation, and quenching are explicitly incorporated in the calculations. The calculated spectra of emitted radiation are in good agreement with measured spectra for several combinations of lamp temperature and mercury composition. Also in agreement with experiments, the addition of $^{196}_{80}$Hg to natural mercury is found to increase lamp efficiency. The method is useful for a number of problems in radiation transfer.

## INTRODUCTION

Radiation emitted by an atom in an optical transition from an excited state to the ground state is commonly called "resonance radiation." Since the absorption of this radiation by atoms in the ground state is typically high, it is unlikely that a quantum of resonance radiation emitted within a chamber containing emitting atoms in the gas phase will reach the walls before being reabsorbed. The absorbing atom may subsequently emit radiation and the emission-absorption steps may be repeated a large number of times. The radiation is described as "imprisoned" or "trapped" when the number of steps required for escape to the walls is large.

Imprisonment of resonance radiation occurs with the 2537-Å line of mercury in the common fluorescent lamp.[1] Mercury atoms excited to the $6\,^3P_1$ state in the low-pressure mercury-argon discharge emit 2537-Å ultraviolet radiation in decaying to the $6\,^1S_0$ ground state. On the average 50—100 emission-absorption steps are required for the radiation to reach the phosphor-coated wall. In the process the excited atoms may be quenched in collisions with ions, atoms or electrons and the radiation may be lost to thermal energy. The effect of imprisonment is to increase the concentration of excited mercury atoms and the probability of quenching and to decrease the efficiency of the lamp.

An early analysis of imprisonment was carried out by Compton[2] who treated the transfer of resonance radiation as a diffusion process. In analogy with the simple kinetic theory description of diffusion in gases the radiation quanta were considered to have a mean free path and a mean lifetime from which a diffusion coefficient could be estimated. Later treatments by Kenty[3] and by Holstein[4] took into account the effects of line shape and the dependence of mean free path upon frequency. Measurements[5–7] of the decay time for optically excited mercury in enclosures of several geometries gave satisfactory agreement with the predictions of Holstein's diffusion treatment. Recently, Alley[8] has presented a more general analytic approach based on the analogy with a random walk.

We report here the development of an alternate method of treating radiation imprisonment based on simple Monte Carlo simulation of the physical processes which occur. The assumptions inherent in the diffusion treatments are eliminated. Collisional transfers of energy are easily incorporated. The results give in detail all the properties of the system including the spectrum of radiation leaving the system and its spatial distribution. The method is tested in its application to the case of the common fluorescent lamp and results are compared with experimental measurements for lamps containing mercury of natural isotopic composition and mercury enriched in the isotope $^{196}$Hg. The variation in lamp efficiency with $^{196}$Hg enrichment is predicted.

## EMISSION AND ABSORPTION OF RESONANCE RADIATION

We use the analysis of Holstein[4] in determining emission line shapes and frequency-dependent absorption coefficients as affected by Doppler and Lorentz (pressure) broadening. For the system of interest natural, Holtsmark, and Stark-effect broadening are small in comparison to the combined Doppler and pressure broadening and are neglected. The text by Mitchell and Zemansky[9] gives a full discussion.

### Emission and collision probabilities

The decay of an excited state by radiation is given by

$$\frac{dN}{dt} = -k_e N = -\frac{N}{\tau} , \tag{1}$$

where the rate constant for emission $k_e$ is related to the lifetime $\tau$ by $k_e = 1/\tau$. In the presence of the competing processes of quenching and collisional transfer with rate

 

constants $k_q$ and $k_t$, the probability of emission is given by

$$P_e=\frac{k_e}{k_e+k_q+k_t} . \tag{2}$$

The probabilities of quenching and transfer are given by similar expressions.

For thermal equilibrium of molecular velocities the rate constant $k_i$ for a collisional process involving an excited atom with molecules $i$ is given by

$$k_i=\left[\frac{8kT}{\pi\mu}\right]^{1/2} S_i n_i , \tag{3}$$

where $k$ is the Boltzmann constant, $T$ is the temperature, $\mu$ is the reduced mass of the colliding species, $n_i$ is the number density of the molecules, and $S_i$ is the cross section (assumed independent of relative velocity) for the process.

### Absorption coefficient

The probability of radiation of frequency $\nu$ traveling a distance $l$ is related to the frequency-dependent absorption coefficient $k(\nu)$ and the mean free path $\lambda(\nu)$ by

$$P(l)=e^{-k(\nu)l}=e^{-l/\lambda(\nu)} . \tag{4}$$

For Doppler broadening only (an ideal reference case) the absorption coefficient is given by

$$k(\nu)=k_0 \exp\left[-\left[\frac{\nu-\nu_0}{\nu_0}\right]^2\left[\frac{c}{v_0}\right]^2\right] , \tag{5}$$

where

$$v_0=(2kT/m)^{1/2} \tag{6}$$

and

$$k_0=\frac{\lambda_0^3 N}{8\pi}\frac{g_2}{g_1}\frac{1}{\pi^{1/2}\nu_0\tau} . \tag{7}$$

Here $\lambda_0$ and $\nu_0$ are the wavelength and frequency for the line center, $m$ is the species mass, $N$ is the number density of absorbing species, $\tau$ is the natural lifetime, and $g_2$ and $g_1$ are the degeneracies of the upper and lower states, respectively.

The combination of Lorentz and Doppler broadening may be expressed by

$$k(\nu)=k_0\frac{a}{\pi}\int_{-\infty}^{\infty}\frac{e^{-y^2}}{a^2+(\omega-y)^2}dy , \tag{8}$$

where

$$a=\frac{\Delta\nu_L}{\Delta\nu_D}(\ln 2)^{1/2} ,$$

$$\omega=\frac{\nu-\nu_0}{\Delta\nu_D}2(\ln 2)^{1/2} ,$$

$$\Delta\nu_L=\frac{1}{\pi}Z_L ,$$

$$\Delta\nu_D=\nu_0\frac{v_0}{c}2(\ln 2)^{1/2} ,$$

and $Z_L$ is the species collision rate. The integral in Eq. (8) is tabulated in Ref. 9 for $a\leq 0.01$. For $a>0.01$ the Voigt profile[10] is convenient:

$$\begin{aligned}
&k(\nu)=k_0\frac{[V(Z)/C]_{a=a,z=z}}{[V(Z)/C]_{a=0,z=0}} ,\\
&W=\frac{a+a^2}{2+a}+0.832\,55 ,\\
&X=\frac{\nu-\nu_0}{\nu_0}\frac{c}{v_0} ,\\
&Z=\frac{X}{W} ,\\
&D(Z)=\exp(-0.693\,15Z^2) ,\\
&L(Z)=\frac{1}{1+Z^2} ,\\
&V(Z)=e^{-(a/1.23)}D(Z)+(1-e^{-(a/1.23)})L(Z) ,\\
&C=[2.128\,39e^{-(a/1.23)}+\pi(1-e^{-(a/1.23)})]W .
\end{aligned} \tag{9}$$

### Emission frequency distribution

For complete thermodynamic equilibrium the probability $P(\nu)$ of emission of a frequency must be proportional to the absorption coefficient for that frequency,

$$P(\nu)\propto k(\nu) . \tag{10}$$

For the system treated the radiation is not in equilibrium with the atoms and the thermodynamic justification of Eq. (10) is not complete. However, Holstein[4] has shown that for Doppler and pressure broadening Eq. (10) is valid and gives the appropriate emission distribution.

## THE STANDARD T12 Hg-Ar FLUORESCENT LAMP

Waymouth[1] has described in detail the physics of mercury–rare-gas fluorescent lamps. In this study we simulated the resonance radiation imprisonment in the standard T12 Hg-Ar lamp because results of measurements[11–13] of the ultraviolet emission spectrum and lamp efficiencies are newly available for several different isoto-

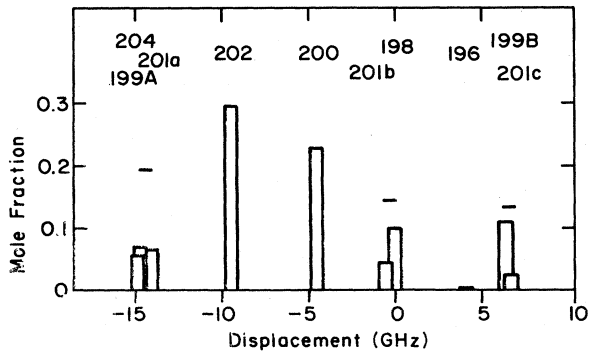


FIG. 1. Hyperfine structure of the 2537-Å line for mercury of natural isotopic composition.

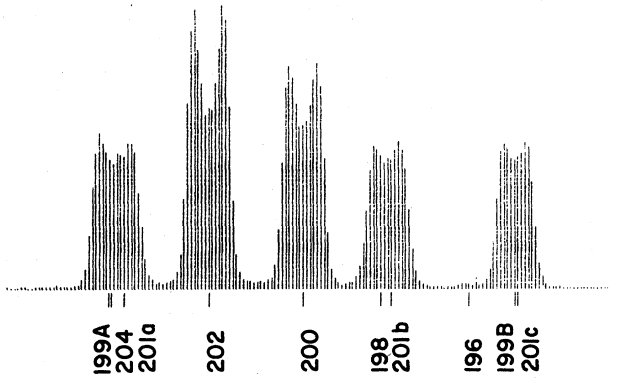


FIG. 2. Calculated exit spectrum (all angles) for natural mercury at wall temperature of 15 °C.

pic compositions of mercury. The output of the lamp is intimately related to the extent of imprisonment.

The T12 Hg-Ar lamp is a tubular lamp 1.5 inches in diameter filled with 2.5 Torr (298 K) of argon and sufficient mercury to saturate the gas. It is operated at a wall temperature of about 313 K so that the mercury pressure is about $6\times10^{-3}$ Torr. The gas (i.e., the Hg and Ar) temperature is about 360 K and the electron temperature is about 11 000 K at the center of the tube. The discharge current is about 425 mA with an arc potential drop of about 105 V in a 4-ft lamp.

The energy balance[1,14] for such lamps shows about 65% of the electrical energy input is released as radiation in the 2537-Å line of mercury. Another 5% is released as radiation at wavelengths not useful in exciting the phosphor wall coating and the balance or 30% is lost as thermal energy to the tube wall. The efficiency of the phosphor in converting energy of 2537-Å radiation into energy at visible wavelengths is about 40%, so that the overall efficiency in converting electrical energy into radiation energy in the visible region is about 25%.

The free electrons in the plasma are accelerated by the electric field and gain energy. They lose energy through elastic and inelastic collisions with gas atoms and the tube wall. Inelastic collisions with the atoms result in either excitation or ionization of the atoms. Once excited the mercury atoms may radiate energy or be quenched in collisions with electrons, atoms or the tube wall. They may also be excited to higher levels or ionized in collisions with electrons.

TABLE I. Stable mercury isotopes, their natural abundance and hyperfine components of the 2537-Å line. Abundance from Bitter, Ref. 15. Hyperfine splittings from Schweitzer, Ref. 16.

| Mass number (amu) | Abundance | Hyperfine splitting ($10^{-3}$ cm$^{-1}$) | Index |
|---|---|---|---|
| 196 | 0.0015 | 137.0±4.0 | 171 |
| 198 | 0.1002 | 0 | 149 |
| 199 | 0.1684 | *A* −514.0±0.4 | 69 |
| | | *B* 224.4±0.2 | 184 |
| 200 | 0.2313 | −160.3±0.2 | 124 |
| 201 | 0.1322 | *a* −489.0±0.3 | 73 |
| | | *b* −22.6±0.1 | 146 |
| | | *c* 229.2±0.5 | 185 |
| 202 | 0.2980 | −337.0±0.2 | 97 |
| 204 | 0.0685 | −510.8±0.4 | 69 |

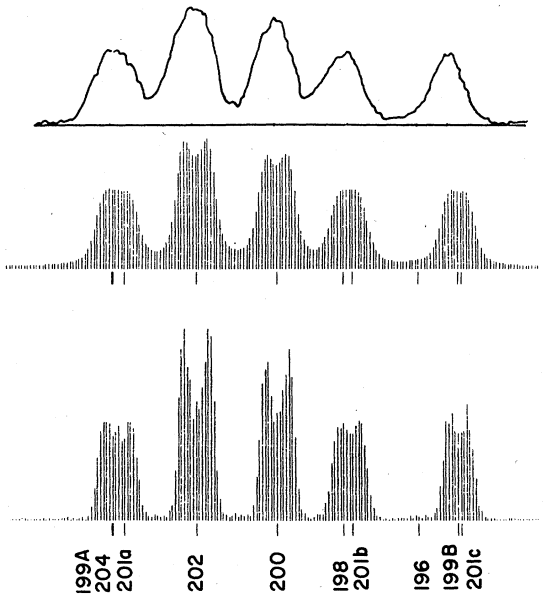


FIG. 3. Narrow angle exit spectra for natural mercury at 15 °C. Lower: calculated. Middle: calculated with resolution factor $f=1100$. Top: experimental from Ref. 13.

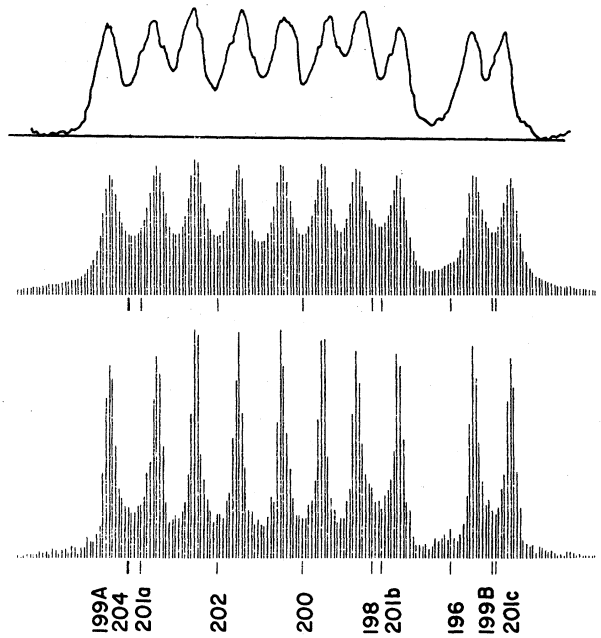


FIG. 4. Narrow angle exit spectra for natural mercury at 40 °C. Lower: calculated. Middle: calculated with resolution factor $f=1100$. Top: experimental from Ref. 13.

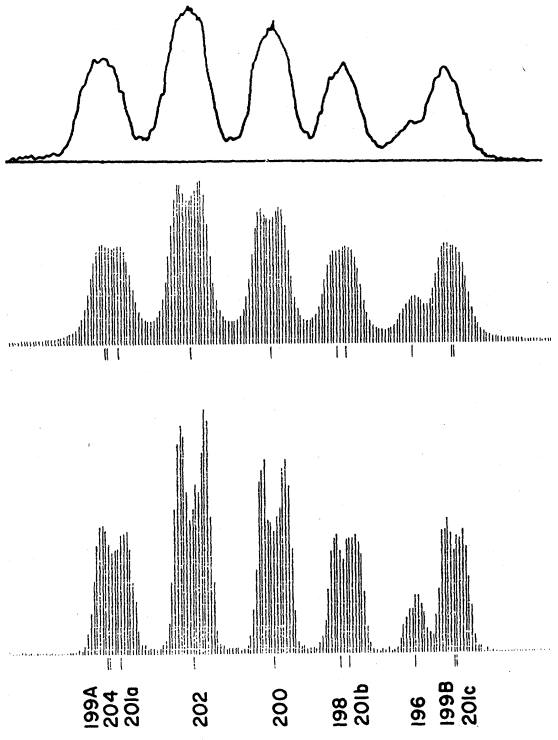


FIG. 5. Narrow angle exit spectra for natural mercury enriched to 4.0% $^{196}$Hg at 15 °C. Lower: calculated. Middle: calculated with resolution factor $f=1100$. Top: experimental (3.9% $^{196}$Hg) from Ref. 13.

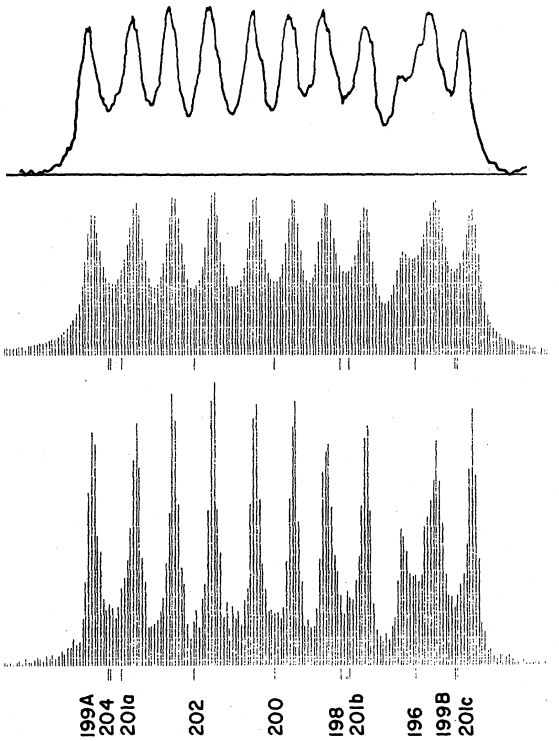


FIG. 6. Narrow angle exit spectra for natural mercury enriched to 4.0% $^{196}$Hg at 40 °C. Lower: calculated. Middle: calculated with resolution factor $f=1100$. Top: experimental (3.9% $^{196}$Hg) from Ref. 13.

The exit of the 2537-Å radiation from the $6\,^3P_1$ state of mercury is facilitated by the presence of seven isotopes occurring in natural mercury. The emission spectrum is separated into five distinct groups of lines with relatively little overlap as shown in Figs. 1 and 2. The line centers and isotope abundances are listed in Table I. Hyperfine splitting of the lines for the odd masses 199 and 201 causes these to be divided among the five groups. The separation into five groups results in a lower imprisonment time for 2537-Å radiation and a higher efficiency for the lamp.

Recent experiments by Grossman *et al.*[11,12] and Maya *et al.*[13] have shown that the efficiency may be improved by varying the isotopic composition of the mercury to reduce imprisonment time. The addition of $^{196}$Hg to natural mercury provides a partially separated sixth group to the spectrum as another route for the escape of the 2537-Å radiation. The lamp efficiency was improved by about 5% (e.g., from 20% to 21% overall) by increasing the concentration of $^{196}$Hg from 0.15% in natural mercury to about 4%. Their measurements[13] of the hyperfine structure of the lamp emission for natural and 196-enriched mercury are reproduced in Figs. 3—6.

The improved efficiency is due in part to the collisional transfer of energy from excited isotopes other than 196 to the 196 isotope. A similar transfer between groups of lines occurs in collisions of the odd isotopes 199 and 201 with electrons and atoms.[17,18] The isotope 199, for example, may transfer from the $f=\frac{1}{2}$ level (199$A$) to the $f=\frac{3}{2}$ level (199$B$), in a collision with an argon atom.

## CALCULATION METHOD

The calculation of radiation and energy transfer is essentially a simulation of the processes occurring in the lamp. Following the initial excitation of a mercury atom its energy (or photon) is tracked from atom to atom until the photon either leaves the system or is lost in quenching. The procedure is repeated thousands of times to obtain a reliable estimate of the overall exit probability and a spectrum of the exit radiation with an acceptable noise level.

Many of the variables required in the calculation are selected at random from appropriately weighted distributions. For example, an initial isotopic species to be excited is selected with a probability proportional to its fraction in the mixture and the direction of emitted photons is selected at random in three dimensions. The frequency of emitted radiation is selected from the Voigt distribution with the line center corresponding to that of the excited atom.

The range of frequencies occurring in the 2537-Å line is divided into several hundred intervals to facilitate the calculation. The temperature of mercury atoms is assumed constant at the volume-weighted average temperature. This corresponds to a simple average of centerline and

wall temperatures. Absorption constants for each frequency interval and the probabilities of absorption of each frequency by each isotope are precalculated and stored.

End effects are neglected. A photon is tracked in three dimensions but the axial position of the absorbing atom is not retained. Changes in position of excited atoms prior to emission, transfer, or quenching are neglected.

### Initial excitation

The radial position for initial excitation is selected with weight proportional to the square of the radius to conform to a parabolic profile peaked at the axis. The ratio of initial radius $r$ to tube radius $R$ could be selected as

$$\frac{r}{R}=N_R^{1/2}\,, \tag{11}$$

where $N_R$ is a random number in the range (0,1). To obtain an evenly distributed set we choose

$$\frac{r_i}{R}=\left[1-\left[1-\frac{N_i-1/2}{N_t}\right]^{1/2}\right]^{1/2} \tag{12}$$

with $N_i$ beginning at unity for the first selection, increasing by one with additional selections, and ending at $N_t$, the total number of initial selections in a calculation.

The selection of initial isotope is made with weighting according to the relative concentrations of each species. The partial sums of species fractions, defined as

$$s_i=\sum_{j=1}^{i} x_j\,, \tag{13}$$

where $x_j$ is the fraction of the total, are used together with a new random number. The isotope selected is the one that meets the criterion

$$s_{i-1}<N_R\leq s_i\,. \tag{14}$$

### Emit, transfer, or quench

For an excited atom at radius $r$ the choice among emission, transfer or quenching is made according to Eq. (2). A new random number $N_R$ is selected and the choice is made according to:

$$\begin{aligned} &0\leq N_R\leq P_e, \text{ emit}\\ &P_e<N_R\leq(P_e+P_t), \text{ transfer}\\ &(P_e+P_t)<N_R\leq(P_e+P_t+P_q), \text{ quench}\,. \end{aligned} \tag{15}$$

### Emission frequency

For both emission and absorption we make use of the Voigt distribution given by Eq. (9). The range of possible frequencies for all isotopes is divided into 250 frequency intervals of width $1.92\times10^8$ sec$^{-1}$. The line centers for the even isotopes and the different states for the odd isotopes are located in the intervals given by the index numbers of Table I. The selection of emission frequency interval is based on deviation from the line center and the probability of a given deviation is proportional to $V(Z)$ of Eq. (9). A cumulative fraction of the total weight is computed for each interval with index $-59$ to $+59$ from the line center and a selection is made with a random number in a manner similar to that for species selection, Eq. (13) and Eq. (14), described above.

In the case of the odd isotopes 199 and 201 the selection of excited states 199 $A$ or $B$ and 201 $a$,$b$, or $c$ is made at random according to the relative equilibrium fractions which depend on the degeneracies of each state. For 199 these fractions are $A(\frac{1}{3})$ and $B(\frac{2}{3})$. For 201 they are $a(\frac{1}{2})$, $b(\frac{1}{3})$, and $c(\frac{1}{6})$.

### Emission direction

The direction of the emitted radiation is selected at random in three dimensions. In polar coordinates of arbitrary orientation the angle is chosen as cos$\Theta$ at random in the interval $(-1,1)$ and the angle $\phi$ is chosen at random in the interval $(0,2\pi)$.

### Radiation free path

To determine the free path for radiation in a frequency interval it is necessary to sum the absorption coefficients. This sum $\sum_{\text{all } i} k_i(\nu)$ and the partial sum $\sum_{j=0}^{i} k_j(\nu)$ for the isotopes are calculated using $k(\nu)$ from Eq. (9) with $k_0$ from Eq. (7). The several states of the odd isotopes are treated as independent species.

The mean free path $\lambda'$ is given by

$$\lambda'=\frac{1}{\sum_{\text{all } i} k_i(\nu)}\,. \tag{16}$$

The free path $l$ is selected according to

$$l=-\lambda'\ln N_R\,, \tag{17}$$

where $N_R$ is random in the interval (0,1).

The absorbing species is chosen with a probability proportional to its weight in the sum of the absorption coefficients for the frequency interval. The species selected is the one for which

$$\frac{\sum_{j=1}^{i-1} k_j(\nu)}{\sum_{\text{all } i} k_i(\nu)}<N_R\leq\frac{\sum_{j=1}^{i} k_j(\nu)}{\sum_{\text{all } i} k_i(\nu)}\,, \tag{18}$$

where $N_R$ is random in the interval (0,1).

### Iteration

Following an initial excitation the path of the energy is tracked through emission, transfer, quenching and absorption until either quenching occurs or the radiation leaves the system. If quenching occurs the process is terminated. After an absorption the position of the absorbing atom is checked to determine if it is within the tube. If within, the process is continued as for an initial excitation from the point of absorption. (It is assumed the collision rates of the odd isotopes are sufficiently high for equilibration among their hyperfine levels.) If the absorbing atom is outside the tube the process is terminated.

TABLE II. Results for the four base cases.

| Hg composition[a] | Natural | | 4.0% $^{196}$Hg | |
|---|---|---|---|---|
| Wall temperature | 15 °C | 40 °C | 15 °C | 40 °C |
| Atom temperature | 313 K | 338 K | 313 K | 338 K |
| Hg density, atoms/cm$^3$ | $2.23\times10^{13}$ | $1.75\times10^{14}$ | $2.23\times10^{13}$ | $1.75\times10^{14}$ |
| | Probabilities | | | |
| Emit, $P_e$ | 0.9901 | 0.9463 | 0.9901 | 0.9463 |
| Transfer, $P_t$ | 0.0060 | 0.0500 | 0.0060 | 0.0500 |
| Quench, $P_q$ | 0.0039 | 0.0037 | 0.0039 | 0.0037 |
| Initial excitations[b] | 1.000 | 1.000 | 1.000 | 1.000 |
| Absorptions | 5.821 | 43.985 | 5.430 | 41.112 |
| Emissions | 6.794 | 44.809 | 6.405 | 41.948 |
| Transfers | 0.042 | 2.360 | 0.041 | 2.238 |
| Quenches | 0.027 | 0.176 | 0.025 | 0.164 |
| Exits | 0.973 | 0.824 | 0.975 | 0.836 |
| Exit probability | 0.9731 | 0.8237 | 0.9747 | 0.8361 |
| ($1\sigma$) | ±0.0001 | ±0.0004 | ±0.0001 | ±0.0004 |

[a]The enriched mercury is that from addition of $^{196}$Hg to natural mercury to obtain a mixture containing 4.0% $^{196}$Hg.
[b]120 000 scaled to unity.

Data are accumulated for thousands of initial excitations. These include the number of emissions, transfers, absorptions, quenches and exits from the tube. The number of exits at each frequency interval, in all directions and within a small angle normal to the tube wall at the exit point, are retained for determining the spectra of the exit radiation.

### Variables

Aside from the usual physical constants the variables to be specified include the lifetime of the $6\,^3P_1$ state of mercury, the emitted wavelength and isotopic splitting, the mercury and argon number densities, the tube radius, and the isotopic composition of the mercury. These values are firm for any particular case. Variables with some uncertainty include the atom temperature (tube wall temperature or higher), the cross section for transfer of excitation between mercury atoms, the quenching rate constant, and the Lorentz broadening parameter $a$ or a cross section for the collision rate $Z_L$ of Eq. (8).

## RESULTS

We have considered four base cases for comparison with the spectra and lamp efficiencies determined by Maya *et al.*[13] for the T12 Hg—Ar lamp. These are for wall temperatures of 15 and 40 °C with natural mercury and with natural mercury enriched to 4.0% $^{196}$Hg. Additional calculations were made to test the sensitivity of the results to several of the uncertain variables and to estimate lamp efficiencies for a number of different isotopic compositions.

The variables specified for the base cases are listed in Table II. The value of the coefficient $a$ for Lorentz broadening was specified as 0.02 for argon at 2.5 Torr as estimated from several measurements.[19] The cross section for mercury-mercury transfers was taken as 1000 Å$^2$, the estimate of Holstein *et al.*[8] The rate constant for quenching was the value found in preliminary calculations to give an exit probability of about 0.8.

The exit spectra for the four base cases, determined from 120 000 initial emissions in each case, are shown in Figs. 2 and 7—9. Additional data are listed in Table II. The effects of imprisonment may be seen to give increased line width and line reversal for the higher mercury densities at a wall temperature of 40 °C. At 15 °C the emission-absorption process occurs an average of about six times for each initial excitation. At 40 °C the average is about forty-five.

For comparison with the experimental measurements of the spectra it is necessary to include the effects of resolution of the Fabry-Perot interferometer used. Grossman[20] has estimated a resolution factor $I$ given by

$$I=\frac{1}{1+f\sin^2(b\,\Delta\nu)}\,, \tag{19}$$

where $\Delta\nu$ is the frequency deviation and the two constants of the apparatus are $f=1100$ and $b=1.0\times10^{-10}$ sec. In

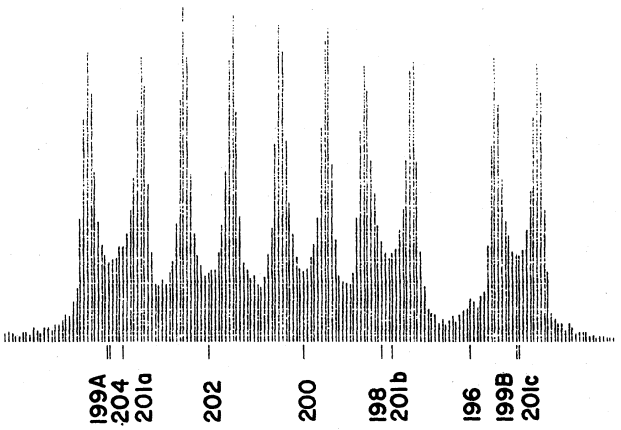


FIG. 7. Calculated exit spectrum (all angles) for natural mercury at wall temperature of 40 °C.

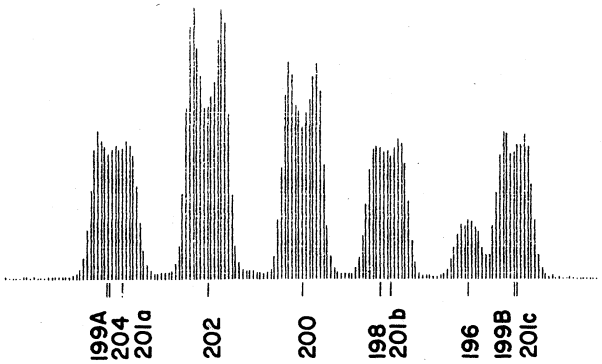


FIG. 8. Calculated exit spectrum (all angles) for mercury enriched to 4.0% $^{196}$Hg at wall temperature of 15 °C.

the experiments the radiation emitted perpendicular to the tube wall from a small spot on the wall was measured. To simulate this we use the calculated spectra of radiation emitted at angles within 20° of perpendicular to the tube wall. Combining the resolution factor with the completely resolved spectra at narrow angles gives the spectra of the four base cases shown in Figs. 3—6. The agreement between calculated and measured spectra is excellent for the two cases at 40 °C but the calculated spectra for 15 °C show a slightly greater line reversal than the measured spectra.

The sensitivities of the spectra to mercury-mercury transfer cross section, Lorentz broadening parameter $a$, quenching rate and initial excitation profile were investigated for mercury enriched to 4.0% $^{196}$Hg. Increasing the mercury-mercury transfer cross section to 5000 Å$^2$ increased the size of the 196 peak by a factor of 2 for 40 °C. Decreasing to zero reduced the 196 peak to about half that for the base case at 40 °C. For 15 °C, the same changes in transfer cross section had only a minor effect. Changing the Lorentz parameter $a$ to 0.04 increased the overlap of groups of lines. Changing $a$ to zero separated the groups in the completely resolved spectra. Reducing the quenching rate to zero had no apparent effect. Replacing the parabolic profile for excitation by a flat profile reduced the quenching probability but the effect on the spectra was minor. Of the several variables only the mercury-mercury transfer cross section and the Lorentz parameter $a$ had a significant effect on the exit spectra.

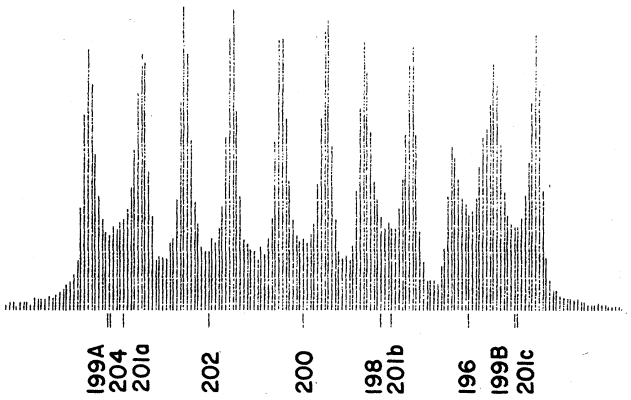


FIG. 9. Calculated exit spectrum (all angles) for mercury enriched to 4.0% $^{196}$Hg at wall temperature of 40 °C.

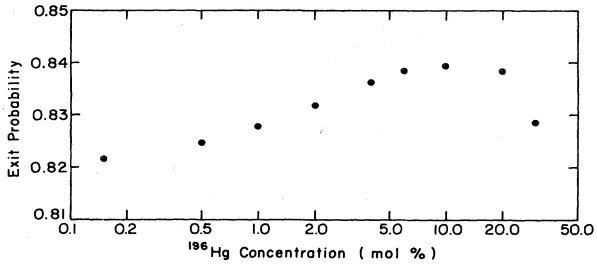


FIG. 10. Variation of overall exit probability with isotopic composition. Natural mercury enriched to $^{196}$Hg fraction indicated.

Additional calculations were made to determine the exit probabilities at various levels of enrichment with $^{196}$Hg. The results are shown in Fig. 10. The exit probability increases with $^{196}$Hg concentration from 82% at zero to a peak of 84% at about 10% $^{196}$Hg and decreases thereafter.

The calculations were performed on a Prime 750 computer programmed in the Fortran language. A typical run of 20 000 initial excitations required about 20 minutes of central processor unit (cpu) time for 40 °C or 3 minutes of cpu time for 15 °C.

## DISCUSSION

The good agreement between calculated and measured spectra, obtained without any adjustment of input parameters, suggests the Monte Carlo treatment gives a faithful simulation of the physical processes involved. It is therefore expected that method may be used successfully in the prediction of many of the properties of systems in which resonance imprisonment occurs. In particular, the effects of several variables on fluorescent lamp performance may be predicted.

The reason for the relatively minor differences in exit line shapes for 15 °C is not clear. The slight line reversal for several groups appearing in the calculated spectra might be explained by a small difference between calculation and experiment in mercury densities. A more likely explanation is that the resolution parameter $f$ for the experiment is lower than that used in modifying the calculated spectra for comparison with experiment. A direct measurement rather than an estimate of the instrument resolution would be useful.

The variation of the exit spectra with exit angle for the four base cases is small. The narrow-angle ( $< 20°$) spectra display a slightly greater line reversal than the spectra for all angles. Since the variation is small the comparison of the narrow angle and experimental spectra (very low angle) appears reasonable.

The method is clearly economical for fluorescent lamps. For systems with much higher absorption probabilities the computation requirements may be excessive. Extension of the technique to treat systems in which the temperatures

or velocity distributions vary with position is relatively simple.

The relation between overall fluorescent lamp efficiency (useful radiation out/electrical energy in) and the overall exit probability reported here (number of exits/initial excitations) is complex[1,21] and not easily determined. The quenching of $6\,^3P_1$ mercury atoms does not necessarily result in the loss of radiation energy to low-temperature heat, since the quenching may release energy to electrons or atoms which return the $6\,^3P_1$ state in subsequent collisions with ground-state mercury atoms. Nevertheless, the relation between imprisonment time and lamp efficiency has been established qualitatively[21] and a similar, but more direct, relation could be developed in terms of exit probability. It is clear that increasing exit probability increases lamp efficiency when other factors are held constant.

The exit probability curve of Fig. 10, calculated for varying mercury-196 concentrations, is similar to the calculated efficacy curve of Ref. 13, which is based on imprisonment time correlations. The shape of the experimental curve of Ref. 13 differs, although the maximum increase in efficiency is similar. Since the experiments are very difficult to perform with high accuracy, the difference may be within the uncertainty in the experimental data.

The method may be applied in the analysis of fluorescent lamps of other configurations and classes. It also has applications in treating a variety of radiative transfer problems including those of other plasmas, laser-excited gases, stellar atmospheres and interstellar space.

---

[1]J. F. Waymouth, *Electric Discharge Lamps* (The MIT Press, Cambridge, Massachusetts, 1971), pp. 11—46.
[2]K. T. Compton, Phys. Rev. **20**, 283 (1922).
[3]C. Kenty, Phys. Rev. **42**, 823 (1932).
[4]T. Holstein, Phys. Rev. **72**, 1212 (1947); **83**, 1159 (1951). See also L. M. Biberman, Sov. Phys.—JETP **19**, 584 (1949).
[5]M. W. Zemansky, Phys. Rev. **42**, 843 (1932).
[6]D. Alpert, A. O. McCoubrey, and T. Holstein, Phys. Rev. **76**, 1257 (1949).
[7]T. Holstein, D. Alpert, and A. O. McCoubrey, Phys. Rev. **85**, 985 (1952).
[8]W. E. Alley, J. Quant. Spectrosc. Radiat. Transfer **30**, 571 (1983).
[9]A. C. G. Mitchell and M. W. Zemansky, *Resonance Radiation and Excited Atoms* (Cambridge University, Cambridge, New York, 1934).
[10]R. Lagushenko (private communication).
[11]M. W. Grossman, S. G. Johnson, and J. Maya, J. Illum. Eng. Soc. **13**, 89 (1983).
[12]M. W. Grossman, R. Lagushenko, and J. Maya, J. Appl. Phys. (to be published).
[13]J. Maya, M. W. Grossman, R. Lagushenko, and J. F. Waymouth, Science **226**, 435 (1984).
[14]M. Koedam, A. A. Kruithof, and J. Riemens, Physica (Utrecht) **29**, 565 (1963).
[15]F. Bitter, Appl. Opt. **1**, 1 (1962).
[16]W. G. Schweitzer, Jr., J. Opt. Soc. Am. **51**, 692 (1961).
[17]S. Mrozowski, Z. Phys. **78**, 826 (1932).
[18]Reference 9, p. 40.
[19]Reference 9, pp. 166—171.
[20]M. W. Grossman (private communication).
[21]J. F. Waymouth and F. Bitter, J. Appl. Phys. **27**, 122 (1956).